

SCIENTIFIC REPORTS



OPEN

NPNT is Expressed by Osteoblasts and Mediates Angiogenesis via the Activation of Extracellular Signal-regulated Kinase

Vincent Kuek^{1,*}, Zhifan Yang^{2,*}, Shek Man Chim^{1,*}, Sipin Zhu^{1,3}, Huazi Xu³, Siu To Chow¹, Jennifer Tickner¹, Vicki Rosen⁴, Wendy Erber¹, Xiucheng Li², An Qin⁵, Yu Qian² & Jiake Xu^{1,3}

Angiogenesis plays an important role in bone development and remodeling and is mediated by a plethora of potential angiogenic factors. However, data regarding specific angiogenic factors that are secreted within the bone microenvironment to regulate osteoporosis is lacking. Here, we report that Nephronectin (NPNT), a member of the epidermal growth factor (EGF) repeat superfamily proteins and a homologue of EGFL6, is expressed in osteoblasts. Intriguingly, the gene expression of NPNT is reduced in the bone of C57BL/6J ovariectomised mice and in osteoporosis patients. In addition, the protein levels of NPNT and CD31 are also found to be reduced in the tibias of OVX mice. Exogenous addition of mouse recombinant NPNT on endothelial cells stimulates migration and tube-like structure formation *in vitro*. Furthermore, NPNT promotes angiogenesis in an *ex vivo* fetal mouse metatarsal angiogenesis assay. We show that NPNT stimulates the phosphorylation of extracellular signal-regulated kinase 1/2 (ERK1/2) and p38 mitogen-activated kinase (MAPK) in endothelial cells. Inhibition of ERK1/2 impaired NPNT-induced endothelial cell migration, tube-like structure formation and angiogenesis. Taken together, these results demonstrate that NPNT is a paracrine angiogenic factor and may play a role in pathological osteoporosis. This may lead to new targets for treatment of bone diseases and injuries.

Angiogenesis is intimately coupled with osteogenesis to mediate bone development, remodelling and repair. An interruption of this coupling process could lead to osteoporosis, a condition commonly caused by aging and post-menopausal oestrogen deficiency¹. For instance, aging mice showed a reduction in CD31^{high} endothelial cells and is associated with a decline in osteoprogenitors and bone volume². In addition, ovariectomised (OVX) mice showed a reduction in bone volume, which is accompanied by a reduction in blood vessels³. Although the inter-relationship between angiogenesis and osteogenesis is critically important, the regulatory factors which mediate this complex process remain poorly understood.

Osteoblasts, osteoclasts and vascular endothelial cells are known to be the main contributors to the remodeling process within a vascularised structure called the bone remodelling compartment (BRC). These cells establish a crosstalk system to mediate bone cell activities and the recruitment, proliferation and differentiation of cells from mesenchymal and haematopoietic lineages^{4,5}. Endothelial cells can regulate bone cells in a paracrine manner via the secretion of macrophage colony-stimulating factor (M-CSF), receptor activator of nuclear factor kappa-B Ligand (RANKL) and various other chemokines^{6–8}. In contrast, osteoblasts produce angiogenic factors such as VEGF, BMP7, EGFL6 and TGF- α to mediate angiogenesis in the bone microenvironment⁹. Furthermore, osteoclasts and preosteoclasts have also been recently implicated in bone formation and angiogenesis by secreting

¹School of Pathology and Laboratory Medicine, University of Western Australia, Nedlands WA 6009, Australia.

²Department of Orthopaedics, Shaoxing People's Hospital, Shaoxing, Zhejiang 312000, China. ³Department of Orthopaedics, The Second Affiliated Hospital, Wenzhou Medical University, Wenzhou, Zhejiang, 325035, China.

⁴Developmental Biology, Harvard School of Dental Medicine, Boston, MA 02115, USA. ⁵Shanghai Key Laboratory of Orthopaedic Implants, Department of Orthopaedic Surgery, Shanghai Ninth People's Hospital, Shanghai Jiao Tong University School of Medicine, Shanghai, China. *These authors contributed equally to this work. Correspondence and requests for materials should be addressed to Y.Q. (email: doctor120@hotmail.com) or J.X. (email: jiake.xu@uwa.edu.au)

MMP-9 and PDGF-BB, respectively^{3,10}. Importantly, angiogenic factors such as VEGF play a crucial role in fracture healing and distraction osteogenesis^{11,12}.

Nephronectin (NPNT) is a 70–90 kDa extracellular matrix protein originally identified in the embryonic kidney¹³. Previous studies report that NPNT is required for kidney and heart development^{14,15}. Furthermore, NPNT was found to promote osteoblast differentiation via EGF-like repeats in MC3T3-E1 osteoblastic cells, and is regulated by TGF- β ^{16,17}. Interestingly, it shares a similar homology with EGFL6, an EGF-like protein which is involved in mediating the proliferation of human adipose tissue-derived stromal vascular cells and angiogenesis^{18–20}. Many EGF-like protein family members such as EGF, HB-EGF and EGFL7 are known to be involved in promoting endothelial cell migration and angiogenesis^{9,21}. Although NPNT contains EGF-like domains, its potential role in mediating angiogenesis in bone and osteoporosis remains to be elucidated. In this study, we examined the expression of NPNT in the bone local environment using *in vitro* and *in vivo* approaches. Furthermore, we characterized the role of NPNT on endothelial cell activities, angiogenesis and the signalling mechanisms involved using *in vitro* functional assays.

Materials and Methods

Cell culture. Osteoclasts were formed by treating primary C57BL/6J mouse bone marrow macrophages (BMM) with recombinant RANKL as previously described²¹. Osteoblasts were formed by culturing primary calvariae cells of neonatal C57BL/6J mice in osteogenic medium according to published protocols^{21,22}. SVEC (a simian virus 40-transformed mouse microvascular endothelial cell line) and COS-7 (a monkey kidney fibroblast cell line) were cultured as previously described²¹.

Real time reverse transcription (RT)-qPCR on osteoblasts. Total cellular RNA isolation and RT-PCR were performed as previously described²³. qPCR amplification was carried out using SYBR green (Qiagen, Australia) and iCycler (BioRad) using the cycling parameters: 94 °C, 1 minute; 60 °C, 30 seconds; 72 °C, 45 seconds for 38 cycles with primers designed against the following mouse sequences: NPNT (forward: 5'-TGGGGACAGTGCCAACCTTCT-3'; reverse: 5'-TGTGCTTACAGGGCCGAGGCT-3'), OCN (forward: 5'-GCGCTCTGTCTCTCTGACCT-3'; reverse: 5'-ACCTTATTGCCCTCCTGCT-3'), Alkaline phosphatase (ALP) (forward: 5'-AACCCAGACACAAGCATTC-3'; reverse: 5'-GCCTTTGAGGTTTTTGGTCA-3'), Col1A1 (forward: 5'-CTGGCGGTTTCAGGTCCAAT-3'; reverse: 5'-TCCAAACCACTGAAGCCTCG-3'), 18S rRNA (forward: 5'-ACCATAAACGATGCCGACT-3'; reverse: 5'-TGTCAATCCTGTCCGTGTC-3'). RT-qPCR results were analysed by ViiA™ 7 Software.

Western blotting. Western blotting was performed as previously described²¹. Immunoreactivity detection and quantification was performed as previously reported^{18,21}. Additional detailed protocols and antibodies' information are provided in the Supplementary Methods.

Transfection and detection of NPNT in COS-7 cells. Transfection was performed according to protocols described previously^{18,21}. Briefly, COS-7 cells were transfected with NPNT expression vector pcDNA3.1-NPNT-c-myc/His or empty pcDNA3.1 vector (control) using lipofectamine 1000 (Invitrogen, Australia). After 6 hours, cells were washed twice and incubated with Opti-MEM reduced serum medium (Gibco). Supernatants were harvested at 24 and 48 hours post-transfection and the presence of NPNT was examined by Western blotting using anti-c-myc antibody.

Mouse ovariectomised model. Female C57BL/6J mice, 5 weeks old, were purchased from Shanghai Super-B&K laboratory animal Corp. Ltd (Shanghai, China). All the animal procedures were approved by the ethics committee (2015/081) of the Shaoxing People's Hospital (Shaoxing, China). Animal experiments were performed in accordance with the approved guidelines. Animals were subjected to the following conditions: normal diet, 20–25 °C room temperature, 50–60% relative humidity, and 12 hours light/dark cycle. After acclimatizing for 2 weeks, mice were divided into sham group or OVX group randomly (6 per group). Mice in the OVX group received ovariectomies bilaterally, and only sham operations were performed in sham group. Animals in both groups were housed for another 3 months post-operation, followed by euthanasia. The forelimbs and femurs were harvested for microCT imaging and RT-qPCR (Supplementary Methods).

Acquirement of patient samples. Ethical approval of all the procedures which involved human subjects was granted by the ethics committee (2015/082) of the Shaoxing People's Hospital (Shaoxing, China). Informed consent was obtained from all the subjects involved, and experimental procedures were carried out in accordance with the approved guidelines. Caput femoris samples were collected from patients who received hip replacement following femoral neck fracture or hip osteoarthritis, and were stored at –80 °C until analyzed. These samples were divided into osteoporosis group (femoral neck fracture) and control group (osteoarthritis) (n = 20) for microCT imaging and RT-qPCR (Supplementary Methods). The detailed information of patients who participated in this study was listed in Supplementary Table 1.

Immunohistochemistry (IHC). The bone sections of mouse tibias were deparaffinised and rehydrated, and incubated with 1% hydrogen peroxidase in methanol for 30 minutes to block endogenous peroxidase activity. Non-specific binding sites were blocked with goat serum for 60 minutes at room temperature before incubation with primary antibody against NPNT (1:600, abcam) or CD31 (1:800, abcam) overnight at 4 °C. For detection, sections were incubated with HRP-conjugated secondary antibody for 60 minutes, followed by the addition of liquid DAB substrate. Sections were counterstained with haematoxylin and were dehydrated and mounted with fast drying mounting media (United Biosciences, Australia). Light microscope and image analysis software (Image plus 6.0) were used and five random regions of each section were taken for statistical analysis of IHC.

***In vitro* angiogenesis assays.** SVEC scratch-wound healing assay, SVEC tube-like structure formation assay and mouse fetal metatarsal angiogenesis assay were performed as previously described²¹. Recombinant mouse NPNT (R&D Systems), human bFGF (PeproTech, Inc.), human VEGF (PeproTech, Inc.) and ERK1/2 inhibitor U0126 (Promega) were purchased for the assays. Ethics approval was obtained from the UWA animal ethics committee (RA/3/100/1331) to carry out the metatarsal angiogenesis assay. Experiments were performed in accordance with the approved guidelines.

Additional detailed protocols are provided in the Supplementary Methods.

Statistical analysis and data presentation. All data were presented as means + SD. For single comparisons, the difference between the two means was evaluated by unpaired, two-tailed Student's t test. For comparison between multiple means, one-way ANOVA was conducted. A level of $P < 0.05$ was considered as statistically significant. Statistical analysis was performed using SPSS software version 19.0. Sample sizes in each animal and patient group were presented as n/group. All *in vitro* data shown represent one of at least three independent experiments.

Results

Gene expression profiles of NPNT during osteoblast and osteoclast differentiation. Previous study has reported that NPNT is expressed by MC3T3-E1 osteoblastic cell line and during the development of long bone and calvaria¹⁶, but its role in angiogenesis and osteoporosis is unknown. In the present study, we performed microarray analysis and found that NPNT is upregulated during primary osteoblast differentiation (day 7), along with the expression of osteoblast marker genes alkaline phosphatase (ALP), osteocalcin (OCN), bone sialoprotein (BSP) and high temperature requirement protease A (HtrA1), a common osteoblast/osteoclast marker²³ (Supplementary Fig. 1A). However, NPNT expression was not altered during RANKL-induced osteoclast differentiation (day 5), whereas osteoclast-associated marker genes calcitonin receptor (CTR), cathepsin K (CtsK), dendritic cell-specific transmembrane protein (DC-STAMP) and HtrA1 were upregulated. Consistent with this observation, further analysis of RANKL-induced osteoclast gene expression by RT-PCR was unable to detect NPNT expression (Supplementary Fig. 1B). Multiple sequence alignment using UniProt (www.uniprot.org) revealed that NPNT's domains are well conserved between mouse and human (Supplementary Fig. 1C). These include a signal peptide sequence at the N-terminus, EGF-like domain sequence, a RGD motif and MAM domain at the C-terminus. Further tree guide analysis also revealed that mouse NPNT is more closely related to human and orangutan NPNT compared to rat NPNT (Supplementary Fig. 1D).

To further investigate the pattern of NPNT gene expression in osteoblasts, we performed RT-qPCR on mRNAs extracted from primary calvarial osteoblasts during differentiation. We showed that NPNT mRNA levels are significantly higher on 7, 14 and 21 days compared to pre-culture with osteogenic differentiation medium on day 0 (Fig. 1A). The differentiation of osteoblasts was confirmed by the upregulation of established osteogenic markers ALP, OCN and alpha-1 type 1 collagen (Col1A1) (Fig. 1B–D).

NPNT is a secreted factor by osteoblasts. Next, we examined osteoblast cell culture for NPNT expression via Western blot analysis. We found that the NPNT protein was present in the supernatant (Fig. 1G) and lysates (Supplementary Fig. 2B), indicating that NPNT is secreted by osteoblasts. Furthermore, an expression construct of mouse full length NPNT (pcDNA3.1-NPNT-c-myc/His) was generated and transiently transfected in COS-7 cells to express NPNT recombinant protein (Fig. 1E). NPNT was detected in the conditioned medium of COS-7 cells 24 and 48 hours post-transfection using anti-c-myc antibody (Fig. 1F), and also in the lysates (Supplementary Fig. 2A). This attested that NPNT is a secreted protein, consistent with other reports that NPNT is an extracellular matrix protein^{13,20}.

NPNT expression was down-regulated in OVX mice and osteoporotic patients. Next, we studied NPNT gene expression using *in vivo* disease models. Firstly, we generated OVX mouse models to mimic the pathological condition post-menopausal osteoporosis in humans (Fig. 2A). In the OVX group at 3 months post-operation, Tb.BV/TV and Tb.N at the proximal tibia were markedly lower than in sham (control) littermates, with Tb.Sp significantly higher in the OVX group (Fig. 2B,D,E). In contrast, no significant difference in Tb.Th was detected between the groups (Fig. 2C). Subsequent RT-qPCR revealed a distinct reduction of NPNT expression in the OVX group (Fig. 2H), along with reductions in the expression of osteogenic markers Runx2 and OCN (Fig. 2E,G).

Next, we examined the NPNT gene expression in the trabecular bone samples obtained from clinical patients (Fig. 2I). Quantitative analysis revealed that Tb.BV/TV and Tb.Th were significantly lower in the osteoporosis group compared to the osteoarthritis (control) group (Fig. 2J,K), while no prominent difference was observed in Tb.N and Tb.Sp between the two groups (Fig. 2L,M). Moreover, RT-qPCR showed that the expressions of NPNT, along with Runx2 and OCN, were significantly lower in the osteoporotic patients in accord with the animal experiment results (Fig. 2N–P).

In addition, we performed immunostaining to examine the protein expression of NPNT and CD31 (an endothelial marker) in the tibias of both sham and OVX mice (Fig. 3A). We found that the protein expression of NPNT was significantly reduced in the tibias of OVX mice, which was consistent with the reduction of NPNT gene expression as described previously (Fig. 3B). Interestingly, we also found that the CD31 expression was significantly lower in the tibias of OVX mice compared to sham mice (Fig. 3C).

Induction of cell migration and tube formation by SVEC endothelial cells and mouse fetal metatarsal angiogenesis by NPNT. Previously, it has been reported that NPNT has sequence homology with EGFL6²⁰. In view of this similarity, we sought to investigate the role of NPNT on endothelial cell activities and angiogenesis. Firstly, we examined the effects of NPNT on SVEC migration by scratch wound healing assay. As

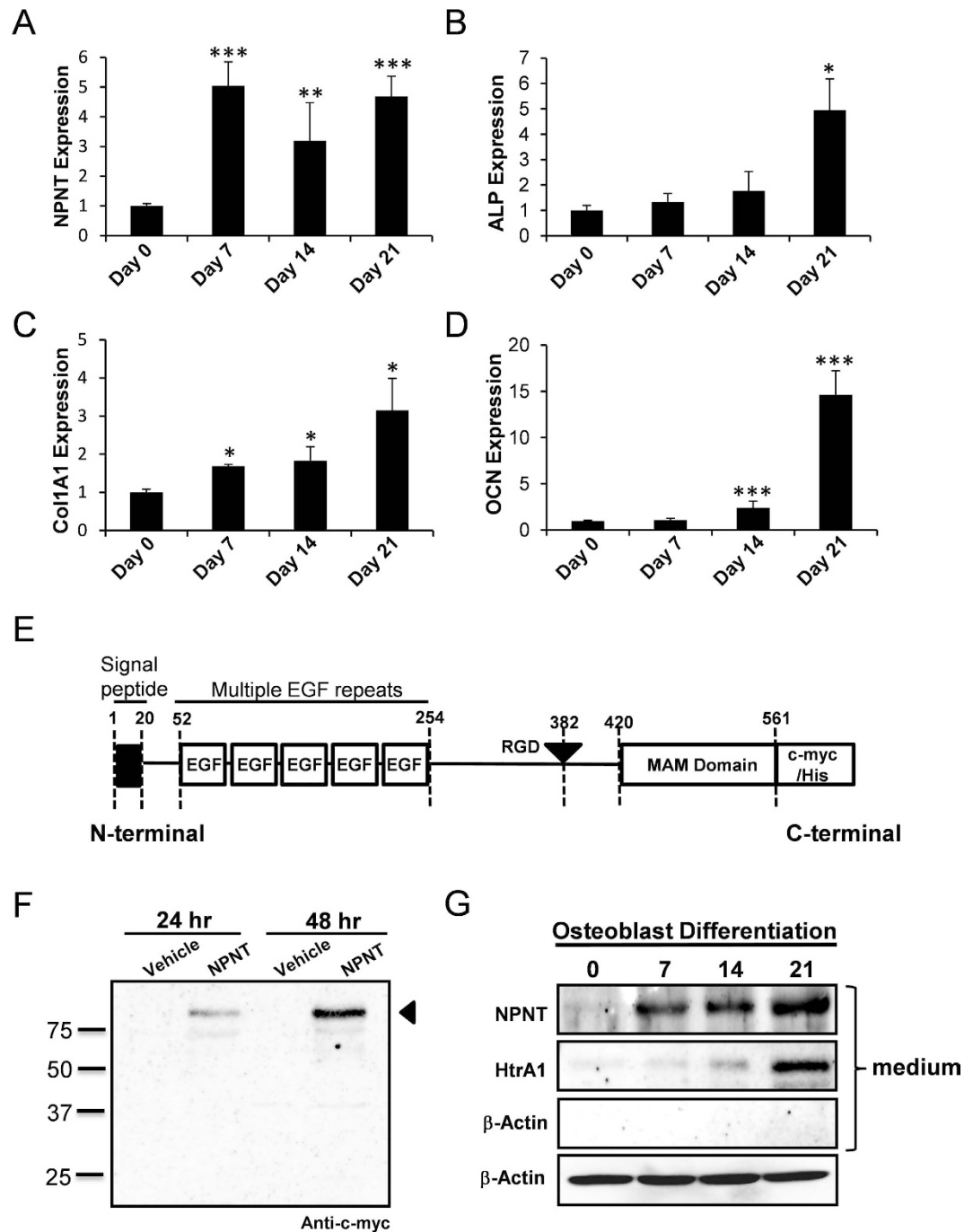


Figure 1. Expression patterns of NPNT in osteoblasts. (A) RT-qPCR was performed during osteoblast differentiation using primers specific for (A) NPNT, (B) ALP, (C) Col1A1, and (D) OCN. Gene expression was normalized to 18S and compared to the expression at day 0. (E) NPNT expression construct (pcDNA3.1-NPNT-c-myc/His), which encodes a mouse full length NPNT, was generated. (F) Detection of NPNT protein in the conditioned medium of COS-7 cells transfected with NPNT expression construct using anti-c-myc antibody. (G) NPNT was detected in osteoblast supernatants using anti-NPNT antibody. HtrA1 was used as positive marker for osteoblast differentiation and β -Actin was used as loading control. Western blot images are presented as cropped format. Full length blots are presented in Supplementary Fig. 4. * $P < 0.05$, ** $P < 0.01$, *** $P < 0.001$.

shown in Fig. 4A,B, exogenous addition of recombinant NPNT protein significantly enhanced endothelial cell migration by ~15% compared to PBS control. bFGF was used as a positive control.

The formation of a three-dimensional tube-like structure is an important step in angiogenesis. Here, we found that recombinant NPNT protein stimulated the formation of tube-like structure by SVEC cells, with the branch

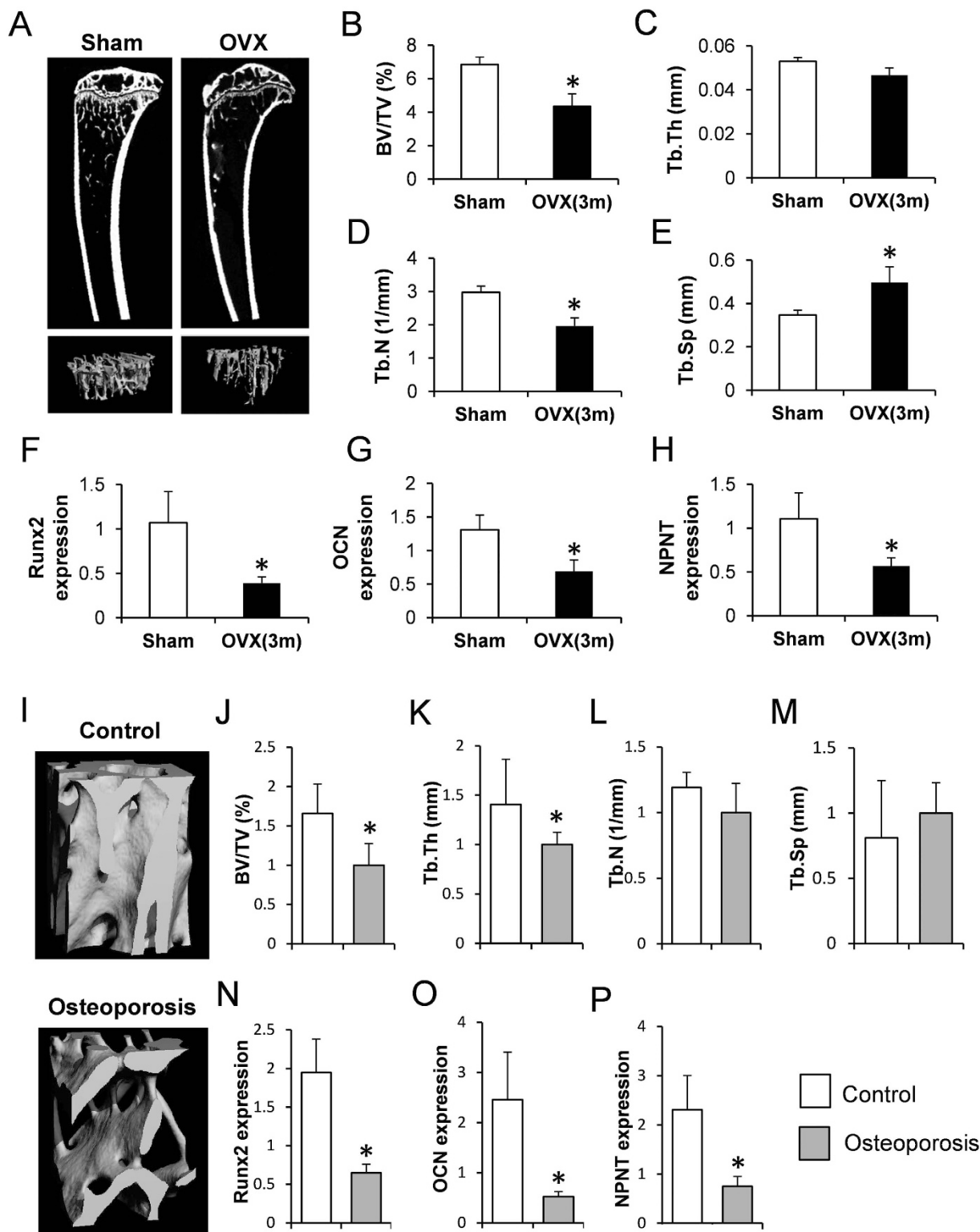


Figure 2. NPNT gene expression was down-regulated in OVX mice and in osteoporotic patients. (A) Tibias from sham group (left) and OVX group (right) were visualized by μ CT scanning, and the ROI focused on the trabecular region below the growth plate for quantitative analysis of (B) Tb.BV/TV, (C) Tb.Th, (D) Tb.N and (E) Tb.Sp. Real-time PCR quantitative analysis of (F) Runx2, (G) OCN and (H) NPNT gene expression in mouse forelimbs. $n = 6/\text{group}$. (I) μ CT images of trabecular bone in the region between head and neck of femur from patients with osteoarthritis (top) and osteoporosis (bottom), and quantitative analysis of (J) Tb.BV/TV, (K) Tb.Th, (L) Tb.N and (M) Tb.Sp. Real-time PCR quantitative analysis of (N) Runx2, (O) OCN and (P) NPNT gene expression in human femora. $n = 20/\text{group}$. The gene expressions were normalized to β -Actin and 18S. * $P < 0.05$.

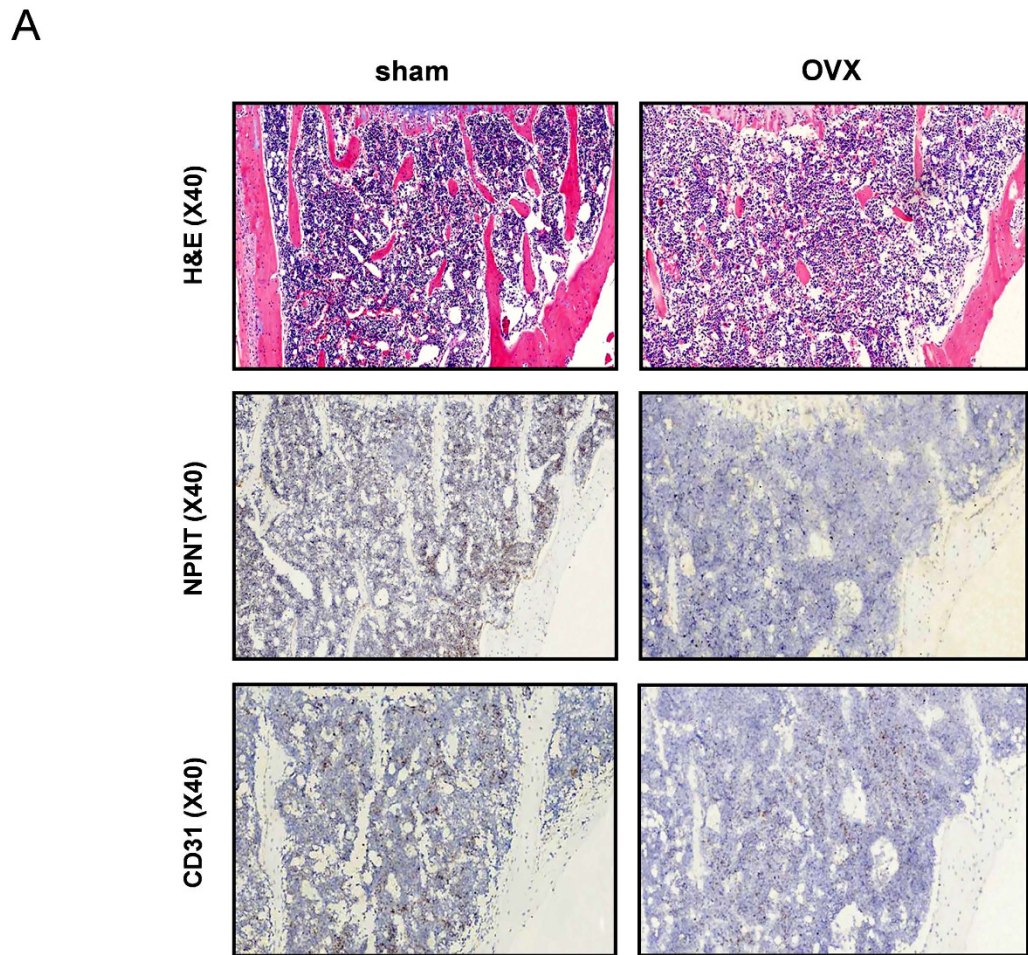
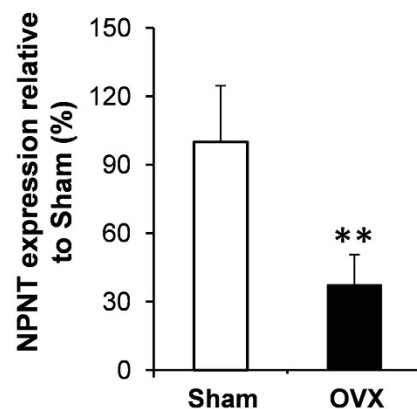
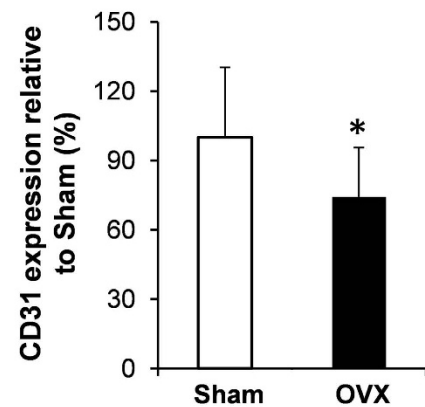
**B****C**

Figure 3. NPNT and CD31 protein expressions were reduced in the tibias of OVX mice. (A) Representative microscopic images of H&E and immunostaining using NPNT and CD31-specific antibody on tibia sections of sham and OVX mice. Quantitative analysis of (B) NPNT and (C) CD31 protein expressions in the tibias of OVX mice. * $P < 0.05$, ** $P < 0.01$.

points and tube lengths significantly enhanced compared to PBS control (Fig. 4C–E). To validate the role of NPNT on angiogenesis, we further performed an *ex vivo* fetal mouse metatarsal angiogenesis assay. As shown in Fig. 4F,G, mouse recombinant NPNT significantly promoted the formation of web-like structures in cultured metatarsals.

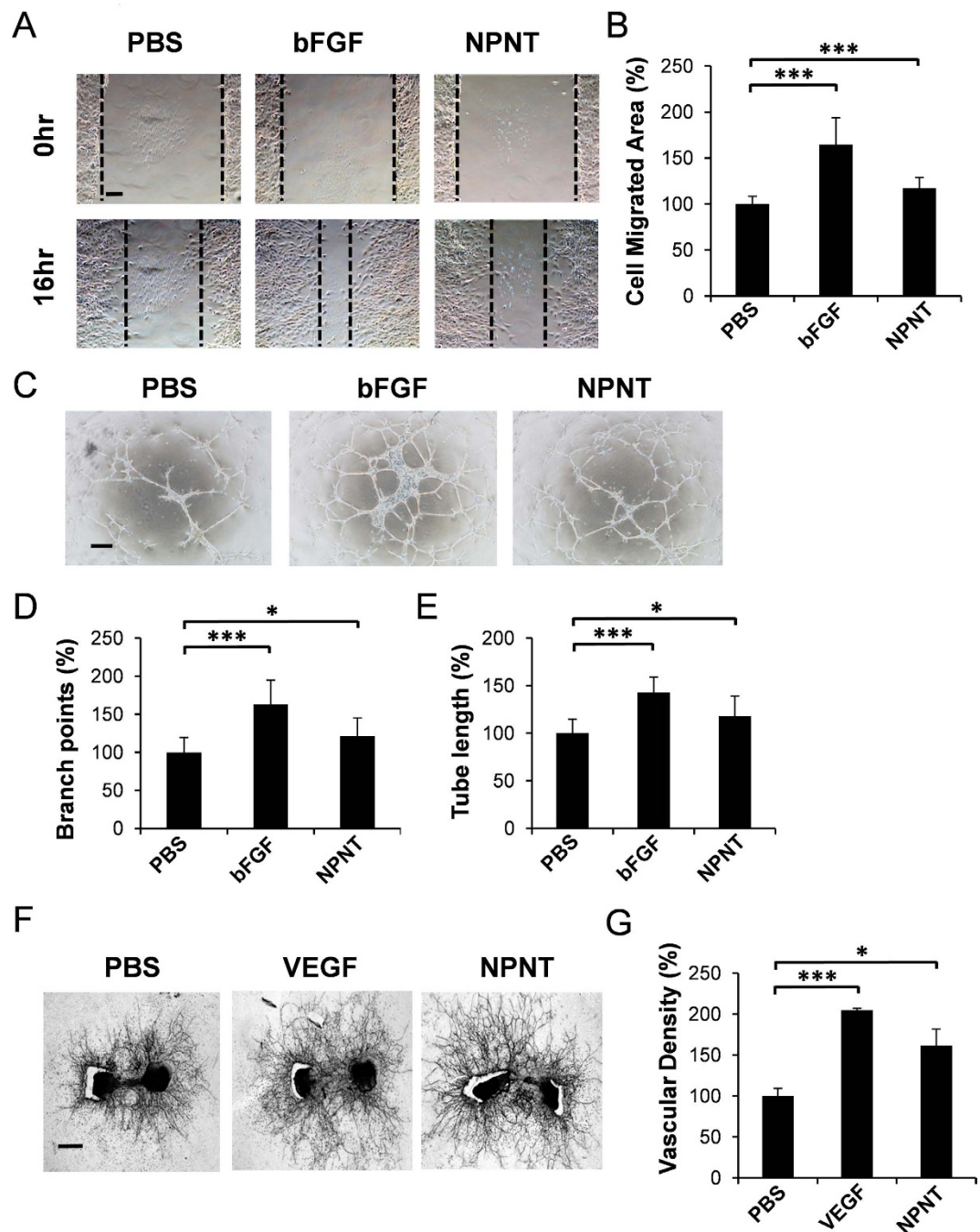


Figure 4. NPNT promotes endothelial cell migration, tube-like structure formation and angiogenesis. (A) Representative microscopic views of scratch wound healing assays performed using SVEC cells treated with recombinant mouse NPNT (500 ng/ml) from 0 to 16 hours. Scale bar, 100 μ m. (B) Quantitative analysis of cell migration area. (C) Representative images showing tube-like structure formation by SVEC cells following treatment with recombinant mouse NPNT (500 ng/ml) for 24 hours. Scale bar, 100 μ m. (D,E) Quantitative analysis of branch points and tube lengths. PBS and bFGF were used as a negative and positive control respectively. (F) Representative images showing that recombinant mouse NPNT (200 ng/ml) induced vessel outgrowth from metatarsals dissected from E17.5 embryos. Scale bar, 250 μ m. (G) Quantitative analysis of vessel sprouting. PBS and VEGF (50 ng/ml) were used as a negative and positive control respectively. * $P < 0.05$, ** $P < 0.01$, *** $P < 0.001$.

NPNT activates ERK1/2 and p-38 signalling pathways. To address the signalling mechanism of NPNT-induced endothelial cell activities, SVEC cells were stimulated with NPNT recombinant protein for 0, 5, 10, 20, 30 and 60 minutes, followed by Western blotting to detect the phosphorylation of key signalling molecules. As shown in Fig. 5A, NPNT induced the phosphorylation of ERK1/2 and p-38, whereas Akt remains relatively

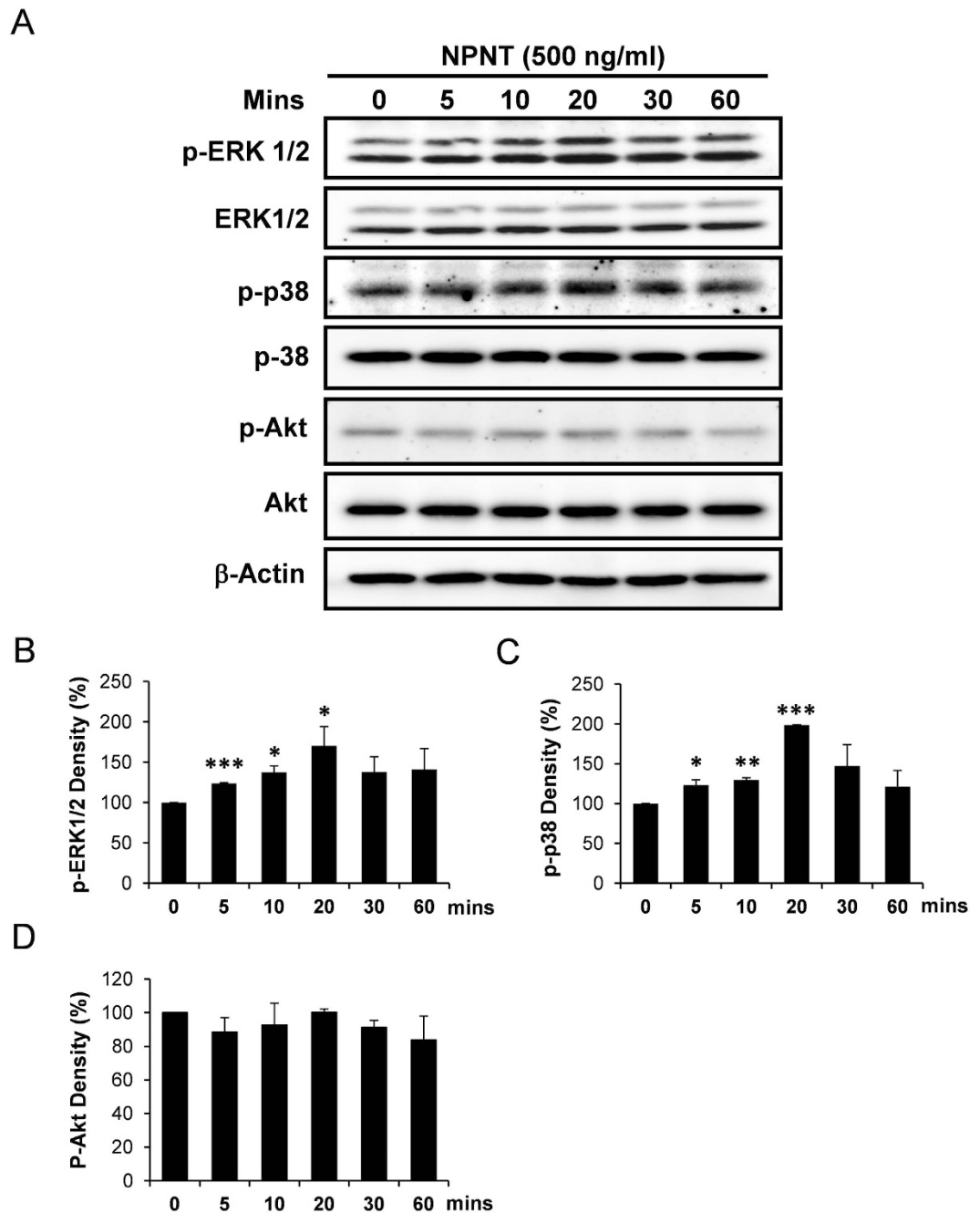


Figure 5. NPNT induced phosphorylation of ERK1/2 and p-38. (A) Western blot images showing the treatment of SVEC cells by mouse recombinant NPNT resulted in the phosphorylation of ERK1/2 and p-38, but not Akt. β -Actin was used as a loading control. (B–D) Quantification of signal intensities of p-ERK1/2, p-p38 and p-Akt by ImageJ. Induction ratios at each timepoint were compared to 0 minute, with p-ERK1/2 normalized to ERK1/2, p-p38 normalized to p-38 and p-Akt normalized to Akt. Western blot images are presented as cropped format. Full length blots are presented in Supplementary Fig. 4. * $P < 0.05$, ** $P < 0.01$, *** $P < 0.001$.

constant. The NPNT-induced phosphorylation of ERK1/2 and p-38 appears to be significantly upregulated compared to pre-stimulation (0 minute), with the levels peaking at 20 minutes (Fig. 5B,C). No significant change in the phosphorylation level of Akt was detected (Fig. 5D).

U0126 impairs NPNT-mediated endothelial cell migration, tube-structure formation and metatarsal angiogenesis. Next, we investigated the effect of U0126 (MEK1/2 inhibitor) on NPNT-mediated endothelial cell functions as previously described^{18,21}. As shown in Fig. 6A–C, NPNT-induced endothelial cell migration and tube-like structure formation was significantly inhibited in the presence of U0126. We also found that NPNT-induced blood vessel formation was significantly reduced in the presence of U0126 (Fig. 6D,E). Treatment with U0126 alone did not have significant effect on angiogenesis as compared to PBS control (data not

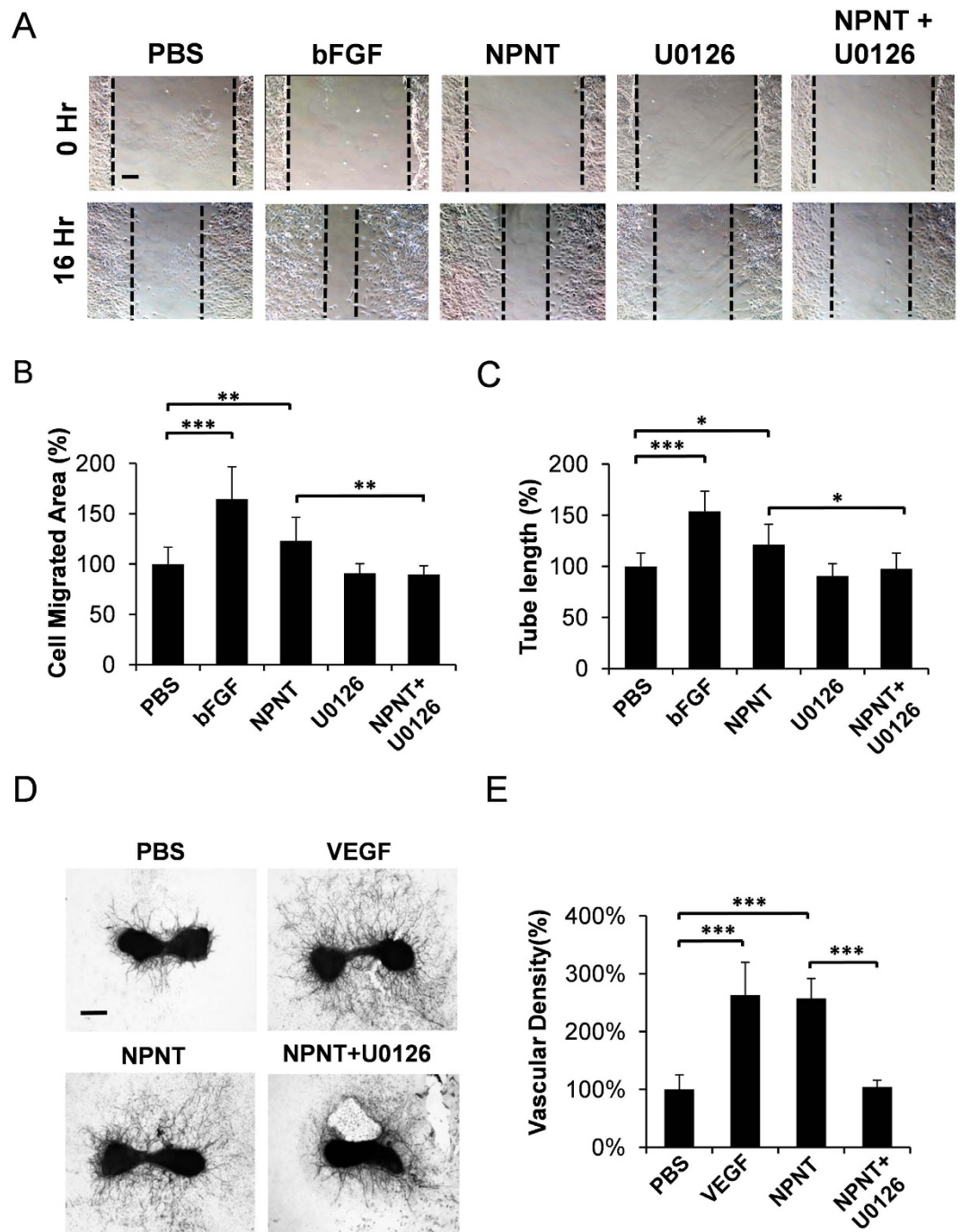


Figure 6. NPNT-induced endothelial cell activities and angiogenesis were inhibited by U0126. (A) Representative microscopic images of scratch wound healing assays showing NPNT-induced endothelial cell migration was blocked in the presence of U0126 (5 μ M). Scale bar, 100 μ m. Quantitative analyses showing that (B) NPNT-induced endothelial cell migration and (C) tube-like structure formation were significantly inhibited by U0126. PBS and bFGF were used as a negative and positive control, respectively. (D) Representative images showing that NPNT-induced angiogenesis was inhibited in the presence of U0126 (5 μ M). Scale bar, 250 μ m. (E) Quantitative analysis of vessel sprouting. * $P < 0.05$, ** $P < 0.01$, *** $P < 0.001$.

shown), consistent with previous study²¹. The inhibition of NPNT-induced ERK1/2 phosphorylation by U0126 in the endothelial cells was confirmed via Western blot analysis (Supplementary Fig. 3).

Discussion

Osteoporosis is often linked to reduced bone quality and increased risk of fracture. Importantly, an association between changes in the vascular architecture and loss of bone mass has been proposed in aged mice², OVX mice³ and human primary osteoporosis²⁴, suggesting that angiogenesis-osteogenesis coupling may be critical

to maintain bone homeostasis. Therefore, identifying novel angiogenic factors in the bone microenvironment could expand our knowledge on the communication between bone cells and endothelial cells, and the roles that they might play in pathological bone diseases. In this study, we have shown that NPNT is expressed and secreted during the differentiation of osteoblasts. Furthermore, we found that the gene expression of NPNT is reduced in femur samples from OVX mice and in osteoporotic femora of humans. Importantly, this observation correlates to a reduction in bone mass and the reduced expression of key osteogenic markers, thus implying that NPNT is at least partly regulated by osteoblasts in the bone microenvironment. We also observed that the reduction of NPNT expression in bone of OVX mice is correlated to a reduction in CD31 expression via immunostaining, thus implying that CD31-expressing cells, including endothelial cells, may be regulated by NPNT.

Previously, our group has demonstrated that EGFL6 and EGFL7 promote angiogenesis^{18,21}. Here, we showed that NPNT can also exhibit angiogenic potential by regulating endothelial cell migration, tube-structure formation and blood vessel growth from mouse fetal metatarsals. Moreover, we found that NPNT could regulate endothelial cell activities and angiogenesis through the activation of ERK1/2 and p38 MAPK signalling pathways. In fact, many EGF-like family members can mediate angiogenesis through the activation of MAPK pathways^{18,25}. Interestingly, NPNT did not affect the phosphorylation of Akt, which plays a crucial role in cell survival and suppression of apoptosis^{26–28}. This result appears to be similar to our previous study which demonstrated that EGFL6 activates ERK1/2, but not Akt signalling pathways in endothelial cells¹⁸. As NPNT shares a very similar structural homology with EGFL6, it is possible that both molecules could regulate angiogenesis in a spatio-temporal manner through similar signalling pathways. NPNT, unlike EGFL6, is a direct target of Wnt/ β -catenin signalling²⁹. NPNT expression is upregulated by Wnt/ β -catenin activation, directly or via inhibition of BMP signaling. Furthermore, deletion of NPNT results in upregulation of EGFL6, thus suggesting a compensatory regulation between the two proteins²⁹. Interestingly, NPNT is expressed in SVEC endothelial cells, but not EGFL6 (data not shown).

EGF-like proteins contain domains which are highly homologous to EGF. This is a common feature among the EGF-like protein family members such as HB-EGF, betacellulin, and amphiregulin⁹. It has been demonstrated that many EGF-like family members are expressed in osteoblasts and osteoclasts⁹, and their roles in regulating angiogenesis have been implicated^{25,30–33}. Therefore, it is possible that NPNT could regulate angiogenesis via the same mechanisms as other EGF-like members. In fact, NPNT contains an RGD motif, which is critical in binding integrins^{13,34,35}. Indeed, NPNT has been reported to be a major ligand for $\alpha_8\beta_1$ integrin, and has lower binding affinities to other integrins such as $\alpha_v\beta_3$, $\alpha_v\beta_5$, $\alpha_v\beta_6$ and $\alpha_4\beta_7$ ¹³. Although the data regarding the presence of $\alpha_8\beta_1$ integrin on endothelial cells is currently lacking, many vascular-related integrin receptors have been reported on endothelial cells, including $\alpha_1\beta_1$, $\alpha_2\beta_1$ ³⁶, $\alpha_v\beta_5$ ³⁷, $\alpha_5\beta_1$ ³⁸ and $\alpha_v\beta_3$ ³⁹. In addition, previous studies have demonstrated that EGFL7, a potent EGF-like angiogenic factor, mediates angiogenesis through the binding of $\alpha_v\beta_3$ integrin and the activation of integrin-associated signalling cascades^{21,40}. Therefore, future studies could explore the possibility that NPNT could regulate endothelial cell activities through integrin interaction.

Many bone diseases have been reported to be associated with disruptions and changes in vascularisation⁹. Furthermore, angiogenesis plays a crucial role during the healing process of bone fractures and growth plate injuries^{41,42}. Therefore, identifying new angiogenic factors may facilitate the development of new therapeutic treatments for skeletal pathologies and injuries. More recently, our group has identified EGFL2, EGFL3, EGFL5, EGFL6, EGFL7, EGFL8 and EGFL9 to be differentially expressed in the bone microenvironment, of which EGFL6 and EGFL7 play an important role in regulating angiogenesis^{18,21}. Our current study presents evidence, for the first time, that NPNT gene expression is affected in osteoporosis and could potentiate angiogenesis *in vitro*. Therefore, it is plausible to postulate that NPNT could mediate the coupling process between angiogenesis and osteogenesis in the bone microenvironment. Future studies will be required to address the *in vivo* role of NPNT in bone using genetically-modified mouse models.

In summary, we have shown that NPNT is expressed by osteoblasts and its expression is reduced in osteoporosis. Furthermore, we also found that NPNT has a direct effect on endothelial cell activities and regulates angiogenesis via p-38 and ERK pathways. This study demonstrates the role of NPNT as a potentially important molecule in the communication between osteoblasts and endothelial cells by a paracrine mode of action. These data may lead to the development of novel therapeutic treatments for bone diseases and fractures.

References

1. Heaney, R. P. Pathophysiology of osteoporosis. *Endocrinol Metab Clin North Am.* **27**, 255–265 (1998).
2. Kusumbe, A. P., Ramasamy, S. K. & Adams, R. H. Coupling of angiogenesis and osteogenesis by a specific vessel subtype in bone. *Nature.* **507**, 323–328 (2014).
3. Xie, H. *et al.* PDGF-BB secreted by preosteoclasts induces angiogenesis during coupling with osteogenesis. *Nat Med.* **20**, 1270–1278 (2014).
4. Kular, J., Tickner, J., Chim, S. M. & Xu, J. K. An overview of the regulation of bone remodelling at the cellular level. *Clin Biochem.* **45**, 863–873 (2012).
5. Sims, N. A. & Vrahnas, C. Regulation of cortical and trabecular bone mass by communication between osteoblasts, osteocytes and osteoclasts. *Arch Biochem Biophys.* **561**, 22–28 (2014).
6. Collin-Osdoby, P. *et al.* Receptor activator of NF- κ B and osteoprotegerin expression by human microvascular endothelial cells, regulation by inflammatory cytokines, and role in human osteoclastogenesis. *J Biol Chem.* **276**, 20659–20672 (2001).
7. Brandi, M. L. & Collin-Osdoby, P. Vascular biology and the skeleton. *J Bone Miner Res.* **21**, 183–192 (2006).
8. Broudy, V. C., Kaushansky, K., Harlan, J. M. & Adamson, J. W. Interleukin 1 stimulates human endothelial cells to produce granulocyte-macrophage colony-stimulating factor and granulocyte colony-stimulating factor. *J Immunol.* **139**, 464–468 (1987).
9. Chim, S. M. *et al.* Angiogenic factors in bone local environment. *Cytokine Growth Factor Rev.* **24**, 297–310 (2013).
10. Cackowski, F. C. *et al.* Osteoclasts are important for bone angiogenesis. *Blood.* **115**, 140–149 (2010).
11. Hu, J. *et al.* Temporospatial expression of vascular endothelial growth factor and basic fibroblast growth factor during mandibular distraction osteogenesis. *J Craniomaxillofac Surg.* **31**, 238–243 (2003).
12. Street, J. *et al.* Vascular endothelial growth factor stimulates bone repair by promoting angiogenesis and bone turnover. *Proc Natl Acad Sci USA* **99**, 9656–9661 (2002).

13. Brandenberger, R. *et al.* Identification and characterization of a novel extracellular matrix protein nephronectin that is associated with integrin alpha 8 beta 1 in the embryonic kidney. *J Cell Biol.* **154**, 447–458 (2001).
14. Linton, J. M., Martin, G. R. & Reichardt, L. F. The ECM protein nephronectin promotes kidney development via integrin alpha 8 beta 1-mediated stimulation of Gdnf expression. *Development.* **134**, 2501–2509 (2007).
15. Patra, C. *et al.* Nephronectin is required for zebrafish heart looping by regulating spatial expression pattern of BMP4. *Circulation.* **120**, S605–S605 (2009).
16. Kahai, S., Lee, S. C., Seth, A. & Yang, B. B. Nephronectin promotes osteoblast differentiation via the epidermal growth factor-like repeats. *FEBS Lett.* **584**, 233–238 (2010).
17. Fang, L. *et al.* Transforming growth factor-beta inhibits nephronectin-induced osteoblast differentiation. *FEBS Lett.* **584**, 2877–2882 (2010).
18. Chim, S. M. *et al.* EGFL6 promotes endothelial cell migration and angiogenesis through the activation of extracellular signal-regulated kinase. *J Biol Chem.* **286**, 22035–22046 (2011).
19. Oberauer, R., Rist, W., Lenter, M. C., Hamilton, B. S. & Neubauer, H. EGFL6 is increasingly expressed in human obesity and promotes proliferation of adipose tissue-derived stromal vascular cells. *Mol Cell Biochem.* **343**, 257–269 (2010).
20. Morimura, N. *et al.* Molecular cloning of POEM: a novel adhesion molecule that interacts with alpha8beta1 integrin. *J Biol Chem.* **276**, 42172–42181 (2001).
21. Chim, S. M. *et al.* EGFL7 is expressed in bone microenvironment and promotes angiogenesis via ERK, STAT3, and integrin signaling cascades. *J Cell Physiol.* **230**, 82–94 (2015).
22. Bakker, A. D. & Klein-Nulend, J. Osteoblast isolation from murine calvaria and long bones. *Methods Mol Biol.* **816**, 19–29 (2012).
23. Wu, X. *et al.* HtrA1 is upregulated during RANKL-induced osteoclastogenesis, and negatively regulates osteoblast differentiation and BMP2-induced Smad1/5/8, ERK and p38 phosphorylation. *FEBS Lett.* **588**, 143–150 (2014).
24. Burkhardt, R. *et al.* Changes in trabecular bone, hematopoiesis and bone marrow vessels in aplastic anemia, primary osteoporosis, and old age: a comparative histomorphometric study. *Bone.* **8**, 157–164 (1987).
25. Mehta, V. B. & Besner, G. E. HB-EGF promotes angiogenesis in endothelial cells via PI3-kinase and MAPK signaling pathways. *Growth Factors.* **25**, 253–263 (2007).
26. Majumdar, A. P. & Du, J. Phosphatidylinositol 3-kinase/Akt signaling stimulates colonic mucosal cell survival during aging. *Am J Physiol Gastrointest Liver Physiol.* **290**, G49–G55 (2006).
27. Gerber, H. P. *et al.* Vascular endothelial growth factor regulates endothelial cell survival through the phosphatidylinositol 3'-kinase/Akt signal transduction pathway. Requirement for Flk-1/KDR activation. *J Biol Chem.* **273**, 30336–30343 (1998).
28. Fujio, Y. & Walsh, K. Akt mediates cytoprotection of endothelial cells by vascular endothelial growth factor in an anchorage-dependent manner. *J Biol Chem.* **274**, 16349–16354 (1999).
29. Fujiwara, H. *et al.* The basement membrane of hair follicle stem cells is a muscle cell niche. *Cell.* **144**, 577–589 (2011).
30. Joyce, N. C., Joyce, S. J., Powell, S. M. & Mekler, B. EGF and PGE2: effects on corneal endothelial cell migration and monolayer spreading during wound repair *in vitro*. *Curr Eye Res.* **14**, 601–609 (1995).
31. Amin, D. N., Hida, K., Bielenberg, D. R. & Klagsbrun, M. Tumor endothelial cells express epidermal growth factor receptor (EGFR) but not ErbB3 and are responsive to EGF and to EGFR kinase inhibitors. *Cancer Res.* **66**, 2173–2180 (2006).
32. Ma, L. *et al.* Antisense expression for amphiregulin suppresses tumorigenicity of a transformed human breast epithelial cell line. *Oncogene.* **18**, 6513–6520 (1999).
33. Kim, H. S. *et al.* Betacellulin induces angiogenesis through activation of mitogen-activated protein kinase and phosphatidylinositol 3'-kinase in endothelial cell. *Faseb J.* **17**, 318–320 (2003).
34. Sato, Y. *et al.* Molecular basis of the recognition of nephronectin by integrin alpha 8 beta 1. *J Biol Chem.* **284**, 14524–14536 (2009).
35. Sanchez-Cortes, J. & Mrksich, M. Using self-assembled monolayers to understand alpha 8 beta 1-mediated cell adhesion to RGD and FEI motifs in nephronectin. *ACS Chem Biol.* **6**, 1078–1086 (2011).
36. Rupp, P. A. & Little, C. D. Integrins in vascular development. *Circ Res.* **89**, 566–572 (2001).
37. Uehara, K. & Uehara, A. Integrin alphavbeta5 in endothelial cells of rat splenic sinus: an immunohistochemical and ultrastructural study. *Cell Tissue Res.* **356**, 183–193 (2014).
38. Suehiro, K., Gailit, J. & Plow, E. F. Fibrinogen is a ligand for integrin alpha5beta1 on endothelial cells. *J Biol Chem.* **272**, 5360–5366 (1997).
39. Brooks, P. C., Clark, R. A. & Cheresh, D. A. Requirement of vascular integrin alpha v beta 3 for angiogenesis. *Science.* **264**, 569–571 (1994).
40. Nikolic, I. *et al.* EGFL7 ligates alpha(v)beta(3) integrin to enhance vessel formation. *Blood.* **121**, 3041–3050 (2013).
41. Glowacki, J. Angiogenesis in fracture repair. *Clin Orthop Relat Res.* S82–S89 (1998).
42. Chung, R. & Xian, C. J. Recent research on the growth plate: Mechanisms for growth plate injury repair and potential cell-based therapies for regeneration. *J Mol Endocrinol.* **53**, T45–T61 (2014).

Acknowledgements

This work was funded in part by National Health and Medical Research Council of Australia, Western Australia Medical & Health Research Infrastructure Fund, Shanghai Pujiang Program (14PJ1406200) and a grant from the National Natural Science Foundation of China (NSFC, no. 81228013). This research was sponsored in part by the Public Project of Zhejiang Province (No. 2014C33150) and Shanghai Pujiang Program (14PJ1406200). Dr. Sipin Zhu is a visiting scholar to UWA sponsored by Wenzhou Medical University, and Dr. Jiakexu made mutual collaborative visits to Wenzhou Medical University from UWA in 2015.

Author Contributions

Conception and design: V.K., S.M.C., Z.Y., Y.Q., A.Q. and J.X. Acquisition and analysis of data: V.K., S.M.C., Z.Y., S.T.C., Y.Q., X.L., A.Q. and J.X. Drafting manuscript: V.K., S.M.C., Z.Y. and J.X. Revising manuscript: V.K., S.M.C., Z.Y., S.Z., H.X., Y.Q., A.Q., J.T., W.E., V.R. and J.X.

Additional Information

Supplementary information accompanies this paper at <http://www.nature.com/srep>

Competing financial interests: The authors declare no competing financial interests.

How to cite this article: Kuek, V. *et al.* NPNT is Expressed by Osteoblasts and Mediates Angiogenesis via the Activation of Extracellular Signal-regulated Kinase. *Sci. Rep.* **6**, 36210; doi: 10.1038/srep36210 (2016).

Publisher's note: Springer Nature remains neutral with regard to jurisdictional claims in published maps and institutional affiliations.



This work is licensed under a Creative Commons Attribution 4.0 International License. The images or other third party material in this article are included in the article's Creative Commons license, unless indicated otherwise in the credit line; if the material is not included under the Creative Commons license, users will need to obtain permission from the license holder to reproduce the material. To view a copy of this license, visit <http://creativecommons.org/licenses/by/4.0/>

© The Author(s) 2016

SCIENTIFIC REPORTS

OPEN **Corrigendum: NPNT is Expressed by Osteoblasts and Mediates Angiogenesis via the Activation of Extracellular Signal-regulated Kinase**

Vincent Kuek, Zhifan Yang, Shek Man Chim, Sipin Zhu, Huazi Xu, Siu To Chow, Jennifer Tickner, Vicki Rosen, Wendy Erber, Xiucheng Li, An Qin, Yu Qian & Jiake Xu

Scientific Reports 6:36210; doi: 10.1038/srep36210; published online 26 October 2016; updated on 21 November 2016

The original version of this Article contained an error in the spelling of the author An Qin, which was incorrectly given as Qin An.

This has now been corrected in the PDF and HTML versions of the Article.

The Author Contributions Statement,

Conception and design: V.K., S.M.C., Z.Y., Y.Q., Q.A. and J.X. Acquisition and analysis of data: V.K., S.M.C., Z.Y., S.T.C., Y.Q., X.L., Q.A. and J.X. Drafting manuscript: V.K., S.M.C., Z.Y. and J.X. Revising manuscript: V.K., S.M.C., Z.Y., S.Z., H.X., Y.Q., Q.A., J.T., W.E., V.R. and J.X.

now reads:

Conception and design: V.K., S.M.C., Z.Y., Y.Q., A.Q. and J.X. Acquisition and analysis of data: V.K., S.M.C., Z.Y., S.T.C., Y.Q., X.L., A.Q. and J.X. Drafting manuscript: V.K., S.M.C., Z.Y. and J.X. Revising manuscript: V.K., S.M.C., Z.Y., S.Z., H.X., Y.Q., A.Q., J.T., W.E., V.R. and J.X.



This work is licensed under a Creative Commons Attribution 4.0 International License. The images or other third party material in this article are included in the article's Creative Commons license, unless indicated otherwise in the credit line; if the material is not included under the Creative Commons license, users will need to obtain permission from the license holder to reproduce the material. To view a copy of this license, visit <http://creativecommons.org/licenses/by/4.0/>

© The Author(s) 2016